

Sebastian WIDZ\*

## **PARTIAL VOLUME EFFECT DETECTION IN MRI SEGMENTATION BASED ON APPROXIMATE DECISION REDUCTS**

Segmentation of Magnetic Resonance Imaging (MRI) is a process of assigning tissue class labels to voxels. One of the main sources of segmentation error is the partial volume effect (PVE) which occurs most often with low resolution images – with large voxels, the probability of a voxel containing multiple tissue classes increases. We propose a multistage algorithm for segmenting MRI images with a mid-stage of recognizing the PVE voxels. The information about PVE regions added to other voxels features extracted from the image can increase the overall accuracy of the segmentation. In our methods we have utilize a classification approach based on approximate decision reducts derived from the data mining paradigm of the theory of rough sets. An approximate reduct is an irreducible subset of features, which enables to classify decision concepts with a satisfactory degree of accuracy in the training data. The ensembles of best found reducts trained for appropriate approximation degrees are applied to detection of the PVE and performing the segmentation.

### 1. INTRODUCTION

Image segmentation is a process of assigning the class labels to data containing spatially varying information. In this article we focus on a Magnetic Resonance Imaging (MRI) of human brain imaged through the series of 2D slices sampled at a particular thickness and resolution. High slice thickness and low image resolution may lead to one of the main sources of error in MRI segmentation called partial volume effect (PVE). PVE occurs when image voxel represents more than one tissue type - when the size of a voxel increases the probability of a voxel containing multiple tissue classes increases. It is expected that solving the PVE issue would increase the MRI segmentation results.

In our approach we create a decision table with objects corresponding to voxels and decisions derived from the Simulated Brain Database (SBD) provided by Montreal Neurological Institute [2,3,5,6] of fully segmented images. SBD contains 3D volumetric multi-spectral images (T1, T2, PD) with axial orientation. Various data sets are available with varying slice thickness from 1mm to 9mm. Figure 1 and Figure 2 present an example of 3mm and 9mm slices imaged in three modalities together with the map matching the PVE regions on the image. One can notice that the amount of PVE is larger on 9mm slice. In our previous work [18] it was stated that when dealing with high level PVE images a higher degree of approximation should be used in the classification process. In this research we use best found parameters from our previous research.

---

\* Polish – Japanese Institute of Information Technology, Koszykowa 86, 02-008 Warszawa, Poland

In proposed segmentation methods we have utilized a classification approach based on approximate reducts derived from the data mining paradigm of the theory of rough sets. An approximate reduct is an irreducible subset of features, which enables to classify decision concepts with a satisfactory degree of accuracy in the training data. The ensembles of best found reducts trained for appropriate approximation degrees are applied to classification of tissue type represented by a voxel. We propose a multistage segmentation algorithm for segmenting human brain MRI Images. In the first stage the PVE identification process is performed, originally proposed in [17]. The results of the PVE identification are then used as an additional feature (attribute) in the final segmentation stage.

The paper is organized as follows: In Section 2, we describe data preparation i.e. feature extraction methods that were applied to MRI images. Section 3 presents foundations of the applied approximate attribute reduction methods. Section 4 reports experimental results. Finally in Section 5 we conclude our research.

## 2. DATA PREPARATION

The magnitudes of MRI images are given in three modalities T1, T2, PD as presented on Figure 1 and 2. Under normal circumstances, the magnitudes of voxels form Gaussian distributions corresponding to the following tissue classes: bone and background (BCG), Cerebrospinal fluid (CSF), Grey Matter (GM), White Matter (WM), and others (fat, skin, muscle). In this work we focus on CSF, GM, and WM.

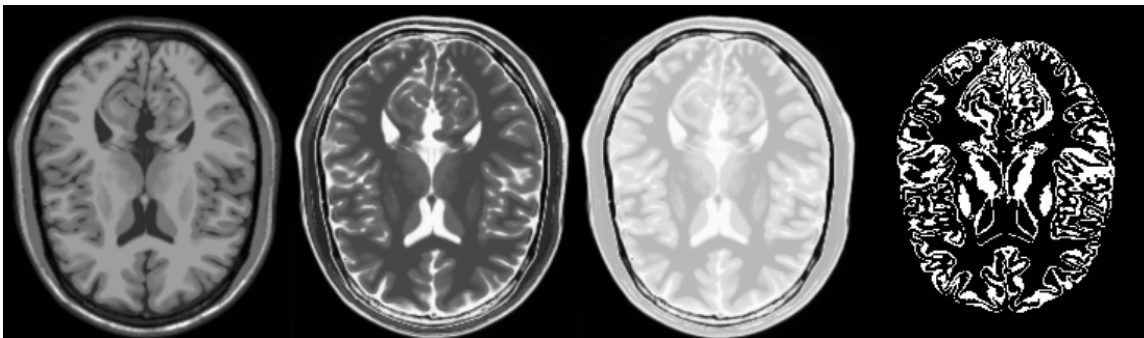


Fig.1. MRI Modalities (from left) T1, T2, PD and PVE region map (3mm slice thickness)

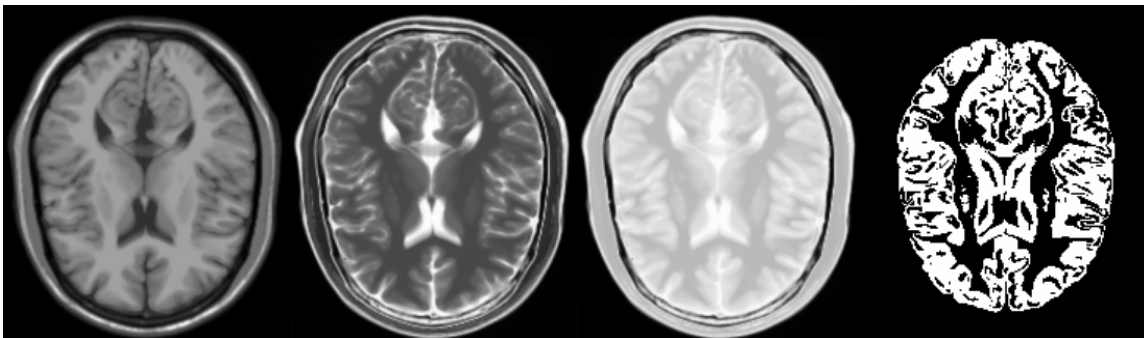


Fig.2. MRI Modalities (from left) T1, T2, PD and PVE region map (9mm slice thickness)

To develop the segmentation, we first generate the training data. Following the standards of the theory of rough sets [8,9], we form a decision table  $IS=(U,A)$ , where each

attribute  $a \in A$  is a function  $a:U \rightarrow Va$  from the universe  $U$  into the value set  $Va$ . The elements of  $U$  are voxels. The set  $A$  contains voxel attributes extracted for each modality. Below we characterize the method we employ to extract the attributes in  $A$  from the MRI images.

EDGE attributes are denoted by  $edge\_T1$ ,  $edge\_T2$ ,  $edge\_PD$ . They are derived using a simple Discrete Laplacian method - a general non-directional gradient operator determining whether the neighborhood of a voxel is homogenous. For instance,  $edge\_T1$  takes the value 0 for a given voxel, if its neighborhood for T1 is homogeneous, and 1 otherwise.

MAGNITUDE attributes are denoted by  $hcMag\_T1_x$ ,  $hcMag\_T2_x$ ,  $hcMag\_PD_x$ ,  $somMag\_T1$ ,  $somMag\_T2$ ,  $somMag\_PD$ . They are derived using the histogram clustering algorithm HCLUSTER [16] (prefix *hc*) and self-organizing map SOM (prefix *som*) for all three image modalities. The index  $X$  used with '*hc*' attributes denotes the number of clusters created by the algorithm. We generate *hc*-attributes based on four and five clusters. SOM and HCLUSTER perform the unsupervised segmentation of the image. The results of such segmentation are recorded as the corresponding attribute values.

NEIGHBOR attributes are denoted by  $hcNbr\_T1_x$ ,  $hcNbr\_T2_x$ ,  $hcNbr\_PD_x$ , as well as  $somNbr\_T1$ ,  $somNbr\_T2$ ,  $somNbr\_PD$ . They are derived from the EDGE and MAGNITUDE attributes. If the edge is not detected for a given voxel, the neighbor attribute's value is copied from the magnitude attribute. Otherwise, it is equal to the magnitude attribute's value occurring more frequently within the direct voxel's neighborhood. Naturally, for *hc*-attributes we use the class values derived from the HCLUSTER algorithm, and for *som*-attributes - those provided by SOM. For example, the value of  $hcNbr\_T1_4$  is calculated from  $edge\_T1$  and  $hcMag\_T1_4$ .

MASK attribute, denoted by  $msk$ , is a rough estimation of the position of a voxel within the slice of the brain. The procedure of creating the mask is the following: first, the brain region is extracted from the image, then the central point of the region is calculated, the region is divided onto four parts by two orthogonal lines crossing in the center. Then three translations are made of all four parts towards by 10, 20 and 50 voxels towards central point. It yields concentric circles defining the position of a voxel. The values of  $msk$  are defined by membership of voxel to particular region.

PVE attribute, denoted by  $isPVE$ , is a binary attribute that holds information about recognizing a voxel as PVE-voxel or noPVE-voxel. At the first stage of the segmentation (PVE identification) all values of this attribute are the same. The result of PVE identification updates the decision table with is then used in segmentation process. Please refer to the next section for a detailed explanation of the whole process.

Attribute  $d \notin A$  indicating the decision attribute is derived from the phantom images taken from SBD. In the PVE identification stage of the  $d$  indicates whether PVE appears on a voxel or not. This information is derived from so called fuzzy phantoms taken from SBD data, where each voxel is labeled with memberships to particular tissue types. We use the

threshold to decide whether a given voxel belongs to noPVE class (if its membership to one of tissues exceeds enough the average tissue content level for the given slice) or to PVE class (if memberships are not diversified enough to decide). The threshold was tuned over the middle brain 3mm slice to get approximately 30%/70% distribution between the PVE and noPVE classes.

In the segmentation stage attribute  $d \in A$  indicates the tissue class label and is derived from the same fuzzy phantom image. Values of  $d \in A$  are labels taken from the phantom corresponding to the tissue with highest volume within a particular voxel.

### 3. APPROXIMATE DECISION REDUCTS

When modeling complex phenomena, a balance between accuracy and computational complexity should be obtained. This balance can be achieved through the use of a *decision reduct*: an irreducible subset  $B \subseteq A$  determining  $d$  in decision table  $IS=(U,A \cup \{d\})$ . The obtained decision reducts are used to produce the decision rules from the training data. Reducts generating smaller number of rules seem to be better as the corresponding rules are more general and applicable. Higher generality and applicability of a rule will contribute to higher accuracy in the classification process as such rules tend to be more insensitive to noise existing in the data. Sometimes it is better to remove more attributes to get even shorter rules at the cost of their slight inconsistencies. One can specify a measure  $M(d/\cdot):P(A) \rightarrow R$  which evaluates the degree of influence  $M(d/B)$  of subsets  $B \subseteq A$  on  $d$ . Then one can decide which attributes may be removed from  $A$  without a significant loss of accuracy. Given  $IS=(U,A \cup \{d\})$ , accuracy measure  $M(d/\cdot)$ , and approximation threshold  $\varepsilon \in [0,1)$ , let us say that  $B \subseteq A$  is an  $(M,\varepsilon)$ -approximate decision reduct, if it satisfies inequality  $M(d/B) \geq (1-\varepsilon)M(d/A)$  and none of its proper subsets does it. For advanced study on such reducts we refer the reader to [10,13]. In the reduct calculation process the *Multi-decision relative gain measure* [15] was used:

$$R(d/B) = \frac{1}{card(U)} * \sum_E P(E) * \max_X \frac{P(X/E)}{P(X)} \tag{1}$$

where  $X \subseteq U$  is a target event (subset),  $E$  is an elementary set, assigned to a conditional probability  $P(X/E)$

$$P(E) = card(E) / card(U) \tag{2}$$

$$P(X) = card(X) / card(U) \tag{3}$$

$$P(X/E) = card(X \cap E) / card(E) \tag{4}$$

and *card* denotes the cardinality function. Measure  $R(d/B)$  expresses the average gain in determining decision classes under the evidence provided by the rules generated by  $B \subseteq A$  [14,15]. Given approximation threshold  $\varepsilon$ , let us say that  $B \subseteq A$  is an  $(R,\varepsilon)$ -approximate decision reduct, if and only if it satisfies inequality

$$R(d/B) \geq (1-\varepsilon)R(d/A) \quad (5)$$

and none of its proper subsets does it.

*Multi-decision relative gain measure* can be used, e.g., to evaluate the potential influence of a particular attributes on the decision. The quantities of  $R(d/\{a\})$ ,  $a \in A$ , reflect the average information gain obtained from one-attribute rules. They are, however, not enough to select the *subsets* of relevant attributes. For instance, several attributes  $a \in A$  with low values of  $R(d/\{a\})$  can create together a subset  $B \subseteq A$  with high  $R(d/B)$ .

The problems of finding approximate reducts are generally hard [10]. Therefore, for the decision table with attributes described in the previous sections, we prefer to consider the use of a heuristic rather than an exhaustive search. We adapt the *order based genetic algorithm* (*o-GA*) searching for minimal decision reducts [19] to find heuristically (sub)optimal  $(R, \varepsilon)$ -approximate decision reducts. We follow the same way of extension as that proposed in [13], also used by ourselves in the previous papers on MRI segmentation [16, 17, 18]. As a *hybrid algorithm* [7], the applied o-GA consists of two parts:

1. *Genetic part*, where each chromosome encodes a permutation of attributes
2. *Heuristic part*, where permutations  $\tau$  are put into the  $(R, \varepsilon)$ -REDORD algorithm described in [13, 20].

#### 4. RESULTS OF EXPERIMENTS

The SBD phantoms have a complete set of MRI volumes, including partial voxel volumes (fuzzy phantoms) of varying slice thickness (3 - 9 mm). For this study, 3mm and 9mm thick volumes were employed. A range of slices from the center of the volume for training/testing purposes was selected.

In the PVE identification step reducts and rules were generated from the training set. Using the derived rule set an identification of the PVE regions was performed. The identification result was then used as a source for *isPVE* attribute in the decision table, and the decision values were substituted with the tissue class labels taken from the fuzzy phantom as described in the Data Preparation section. In the segmentation step the new decision table was used again for generation of reducts and rules.

Reducts and rules were generated always using one slice chosen randomly from the SBD database, for slice range  $\langle 27; 36 \rangle$  for 3mm and  $\langle 7; 15 \rangle$  for 9mm 0% noise and 0% INU (bias field inhomogeneities) The resulting classifier was tested against eight slices (always different than those chosen for training) from the same range. The segmentation becomes more challenging when applied to images representing thicker slices as the number of voxels with PVE is proportional to slice thickness. Figure 3 presents the average (for 8 experiments repeated with different training/testing slices) accuracy (the number of correctly recognized voxels divided by the total number of voxels).

Both results are compared – without embedding the PVE identification stage and using the multistage segmentation process (with PVE identification). For the 1mm data only the crisp data are available (no PVE effect) so only the previously proposed segmentation algorithm could be performed. One can notice that adding the PVE identification step increases the overall accuracy.

Slice Thickness	Accuracy without PVE ident.	Accuracy with PVE ident.
1 mm	98 %	N/A
3 mm	89%	91%
9 mm	81%	86%

Fig.3. Comparison of results obtained using the proposed segmentation algorithm with and without the PVE identification step.

5. FIGURE 4 PRESENTS THE SEGMENTATION RESULTS IN COMPARISON TO IMAGE PHANTOMS USED DURING TRAINING.

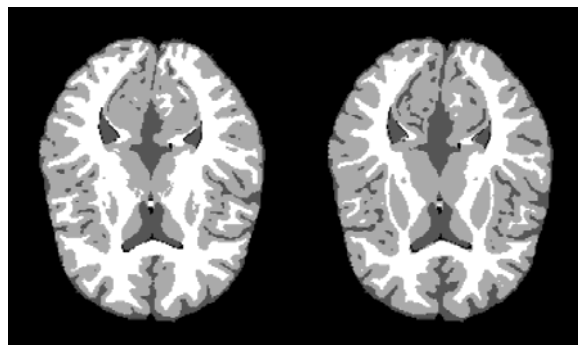


Fig.4. Results of MRI segmentation. 3mm phantom (left) and segmentation result (right).

## 6. CONCLUSIONS

A multistage rough set-based algorithm for brain tissue classification in multi-modal MR images was presented. In comparison to the previous research adding PVE identification to the segmentation algorithm improved the overall accuracy. The results were obtained without any pre-processing such as median filtering or any smoothing operation. Further investigation of the segmentation accuracy, when various pre-processing techniques are embedded into the algorithm, is suggested. In this work multi-modal simulated MRI images were used for training and testing. The reader may refer to our previous work [17] where the similar algorithm was tested on a real-world, single modality (T2) images.

## BIBLIOGRAPHY

- [1] CÁRDENES R, WARFIELD S.K., MACIAS E.M., SANTANA J.A., RUIZ-ALZOLA J., An Efficient Algorithm for Multiple Sclerosis Segmentation from Brain MRI. In: Moreno-Díaz R. and Pichler F., editors, EUROCAST, volume 2809 of Lecture Notes in Computer Science, pp. 542–551. Springer, 2003.
- [2] COCOSCO C.A., ZIJDENBOS A.P., EVANS A.C., Automatic Generation of Training Data for Brain Tissue Classification from MRI. In: Dohi T. and Kikinis R., editors, MICCAI (1), volume 2488 of Lecture Notes in Computer Science, pp. 516–523. Springer, 2002.

- [3] COLLINS D.L., ZIJDENBOS A.P., KOLLOKIAN V., SLED J.G., KABANI N.J., HOLMES C.J., EVANS A.C., Design and Construction of a Realistic Digital Brain Phantom. *IEEE Trans. Med. Imaging*, 17(3): pp. 463–468, 1998.
- [4] DUGAS-PHOClON G., BALLESTER M.Á.G., MALANDAIN G., AYACHE N., LEBRUN C., CHANALET S., BEnSA C., Hierarchical Segmentation of Multiple Sclerosis Lesions in Multi-Sequence MRI. In: *Proceedings of the 2004 IEEE International Symposium on Biomedical Imaging: From Nano to Macro*, Arlington, VA, USA, 15-18 April 2004, pp. 157–160. IEEE, 2004.
- [5] KWAN R.K.S., EVANS A.C., PIKE G.B., An Extensible MRI Simulator for Post-Processing Evaluation. In: Höhne K.H. and Kikinis R., editors, *VBC*, volume 1131 of *Lecture Notes in Computer Science*, pp. 135–140. Springer, 1996.
- [6] KWAN R.K.S., EVANS A.C., PIKE G. B., MRI Simulation Based Evaluation and Classifications Methods. *IEEE Trans. Med. Imaging*, 18(11): pp. 1085–1097, 1999.
- [7] LAWRENCE D.. *Handbook of Genetic Algorithms*. Van Nostrand Reinhold, 1991.
- [8] PAWLAK Z.. *Rough Sets: Theoretical Aspects of Reasoning about Data*. Kluwer Academic Publishers, Norwell, MA, USA, 1992.
- [9] PAWLAK Z., SKOWRON A.. Rudiments of Rough Sets. *Inf. Sci.*, 177(1):pp. 3–27, 2007.
- [10] ŚLĘZAK D., Approximate Entropy Reducts. *Fundam. Inform.*, 53(3-4): pp.365–390, 2002.
- [11] ŚLĘZAK D., Multi-Attribute Dependencies: The Case Study of Association Reducts. Plenary lecture at the International Conference on Rough Sets and Emerging Intelligent Systems Paradigms, RSEISP'2007, Warsaw, Poland
- [12] ŚLĘZAK D., WIDZ S., Approximation degrees in decision reduct classifiers for noisy data. In prep., 2007.
- [13] ŚLĘZAK D., WRÓBLEWSKI J., Order Based Genetic Algorithms for the Search of Approximate Entropy Reducts. In: *Proc. RSFDGrC'2004*, Chongqing, China, pp. 308-311. Springer (2003)
- [14] ŚLĘZAK D., ZIARKO W., Attribute Reduction in the Bayesian Version of Variable Precision Rough Set Model. In: *Proc. of RSKD'2003* Elsevier, ENTCS, 82(4), (2003)
- [15] ŚLĘZAK D., ZIARKO W., The investigation of the Bayesian Rough Set Model. *International Journal Approximate Reasoning*, 40(1-2) pp. 81–91, 2005.
- [16] WIDZ S., REVETT K., ŚLĘZAK D., A Hybrid Approach to MR Imaging Segmentation Using Unsupervised Clustering and Approximate Reducts. In: *Proc: RSFDGrC'2005 (2)*, Regina, Canada, Springer (2005) pp.372–382
- [17] WIDZ S., REVETT K., ŚLĘZAK D., A Rough Set-Based Magnetic Resonance Imaging Partial Volume Detection System. In: *Proc. PReMI'2005*, Calcutta, India, Springer (2005) pp. 756–761.
- [18] WIDZ S. ŚLĘZAK D., Approximation Degrees in Reduct-Based MRI Segmentation, In *Proc: FBIT'2007*, Jeju-Do, Korea, 2007, in publish
- [19] WRÓBLEWSKI J., Theoretical foundations of order-based genetic algorithms. *Fundamenta Informaticae* 28(3-4) pp. 423–430, 1996.

